51st AIAA/ASME/ASCE/AHS/ASC Structures, Structural Dynamics, and Materials Conference
 18th
12 - 15 April 2010, Orlando, Florida

AIAA 2010-2921

Risk Assessment of Scramjet Unstart Using Adjoint-Based Sampling Methods

Qiqi Wang*
Massachusetts Institute of Technology, Cambridge, MA 02139, USA

Karthik Duraisamy†, Juan Jose Alonso‡ and Gianluca Iaccarino§
Stanford University, Stanford, CA 94305, USA

We demonstrate an adjoint based approach for accelerating Monte Carlo estimation of risk, and apply it to estimating the probability of unstart in a SCRamjet engine under uncertain conditions that are characterized by various Gaussian and non-Gaussian distributions. The adjoint equation is solved with respect to an objective function that is used to identify unstart and the adjoint solution is used to generate a linear approximation to the objective function. This linear surrogate is used to divide the uncertain input parameters into three different strata, corresponding to safe operation of the engine, uncertain operation and unstart. The probability of unstart within these strata is very different and as a result, stratified sampling significantly increases the efficiency of the risk assessment procedure by reducing the variance of the estimator. Using this technique, the Monte Carlo method was demonstrated to be accelerated by a factor of 5.4.

I. Introduction

A. Background and Motivation

NASA's X-43 hypersonic vehicle[1] holds the flight speed record among air-breathing propulsion systems, having reached a speed of Mach 10 in 2004. The X-43 is powered by a supersonic combustion (SCRamjet) engine, in which air at supersonic speed is mixed with hydrogen in the combustion chamber. The resulting ignition and explusion of high velocity mixture through the nozzle generates thrust. The SCRamjet is a simple and potentially robust alternative to conventional engines as there are no moving parts. Hypersonic air-breathing vehicles also hold the promise of low-cost access to space and in next generation high-speed transportation. To achieve conditions that enable auto-ignition, the air captured by the engine has to achieve high temperatures and pressures and this is partially accomplished via a sequence of carefully designed shock-waves anchored to the vehicle forebody. The minimum flight speed is, therefore, fixed by the requirement of reaching supersonic flow at the entrance of the SCRamjet (downstream of the forebody compression). On the other hand, the maximum thrust is reached as a direct consequence of optimal mixing and heat release in the combustor and is an increasing function of the fuel flow rate. The design of a SCRamjet system is complicated by the existence of thermodynamic, combustion and fluid-dynamic limits to the amount of fuel that can be burnt in the combustor. The thermodynamic limit is associated with the inability to sustain supersonic flow in a duct with arbitrary heat addition. Above a certain threshold (which is typically referred to as the thermal chocking limit) a normal shock wave is formed in the combustor and the flow becomes

*Corresponding author, Assistant Professor, Aeronautics and Astronautics, Cambridge, MA, USA, AIAA member
†Consulting Assistant Professor, Aeronautics and Astronautics, Stanford, CA, USA, AIAA member
‡Associate Professor, Aeronautics and Astronautics, Stanford, CA, USA, AIAA member
§Assistant Professor, Mechanical Engineering, Stanford, CA, USA, AIAA member

abruptly subsonic. The combustion limit is associated with the stoichiometry of the fuel/air mixture while the fluid-dynamic limit is associated with the blockage induced by the added fuel mass in the chamber and the possibility of creating large areas of flow separation near the injector. It is worth noting that these limits are associated with the critical failures of the system from which it might be impossible to recover.

The performance of a SCRamjet engine is carefully tuned to achieve the highest level of thrust that is compatible with a specified safety margin (the interval between the design condition and a critical failure). Computational tools are routinely used in aerodynamic design and to predict the heat release resulting from combustion[2,3] and these simulations are capable of achieving high levels of accuracy by incorporating detailed representations of the underlying physical processes. The associated computational costs are typically very large and can thus limit the number of configurations can be analyzed. On the other hand, the characterization of the risk relies on the identification of the uncertainties present in the real, operating vehicle and the determination of the corresponding induced variability of the flow conditions within the SCRamjet. A formal reliability analysis requires the determination of the probability of failure of the system which, in turn, involves the analysis of a large number of possible operating scenarios. Thus high-fidelity physics-based computational tools may be rendered infeasible for risk-analysis.

In the present work, a methodology to estimate the probability of unstart of a SCRamjet engine under uncertain conditions is demonstrated. A Monte-Carlo approach is pursued, but the computational cost of the analysis is greatly reduced by applying adjoint-based stratified sampling techniques.

II. Simulation Model

All computations are performed using the unstructured mesh compressible flow solver Joe.[4] While Joe is capable of solving the unsteady Reynolds-Averaged Navier-Stokes equations (RANS) with various combustion and turbulence models, in this work we use its inviscid capabilities with a second-order accurate cell centered discretization for the fluxes. An idealized, two-dimensional version of the HyShot-II scramjet geometry that has been both flight and ground tested[5,6] will be studied. The geometry (Figures 1,2) replicates the isolator, combustor and nozzle of the test vehicle. The inflow to the islolator is approximately at Mach 2.7 and corresponds to the flow *after* it has been deflected by two shocks from the forebody and cowl in the real vehicle. Since the flow entering the simulation domain is the flow downstream of the cowl, the inlet velocity will always be parallel to the combustor walls. Any changes to the vehicle angle of attack will thus translate to changes in the inlet flow variables. A shock train is generated by a blunt lip at the entrance to the lower wall of the isolator as seen in Figure 1. The simulations are run in an inviscid mode and a simple heat release model[7] is used to mimic the combustion process. In this model, the cumulative heat release is simply added as a source term to the energy equation. The heat release (in J/s) is given by:

$$Q = \phi f_{st} H_f m_{air} \eta(x/L_c) \tag{1}$$

where $\eta(x/L_c) = 1 - e^{-(C_c x/L_c)^{D_c}}$ is the heat release distribution function. The various parameters used in the above expressions are summarized in Table 1. The shape parameter D_c is tuned to achieve a good fit with the ground-based experimental measurements of the DLR.[6] The addition of the heat release was seen to accelerate the flow and increase the number of shocks in the combustor (these were also found to be increasing in frequency towards the exit of the combustor). A nominal comparison with experimental data is shown in Figure 3, where the validity of the inviscid model is demonstrated.

III. Discrete Adjoint Formulation for Gradient Computation.

The adjoint procedure[8] is an efficient method to compute the variation of a functional $\mathcal{J}$ with respect to a large number of design parameters. In the *discrete* adjoint approach,[9,10] the adjoint equations are directly derived from the discretized form of the governing equations. Let $R(U, w) = 0$ represent the governing equations in a domain Ω that are to be solved for flow variables U in the presence of one or more uncertain parameters w. We are interested in the values of a functional $\mathcal{J}(U, w)$ and their variations with respect to the parameters w. As will be explained later in this paper, the value of the gradient vector of this functional

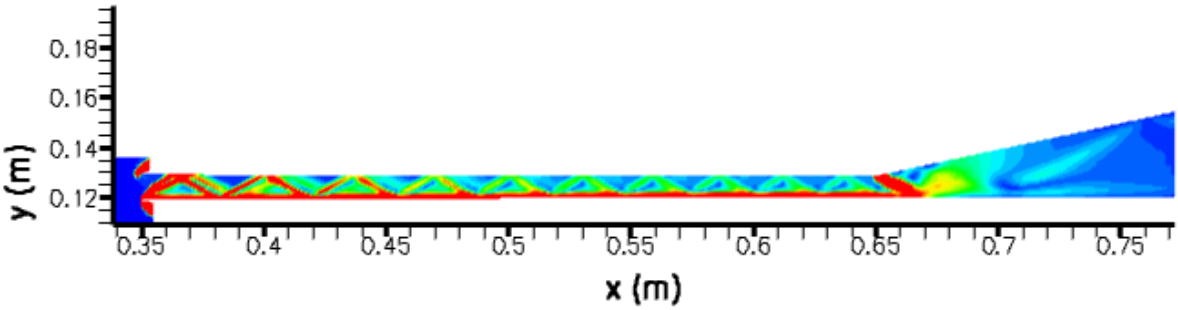

Figure 1. *Simulation domain for HyShot-II SCRamjet. Contours of density gradient magnitude are shown for a case with fuel injection.*

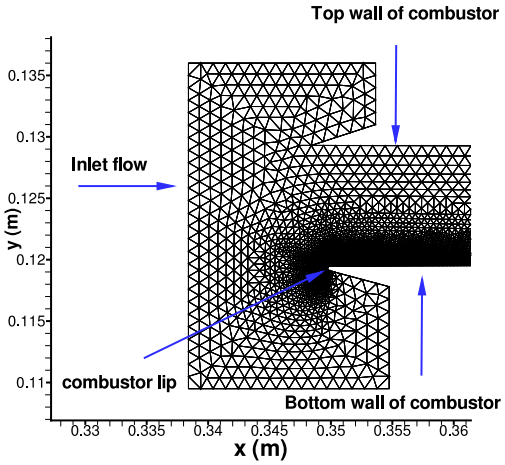

Figure 2. *Mesh near the inlet.*

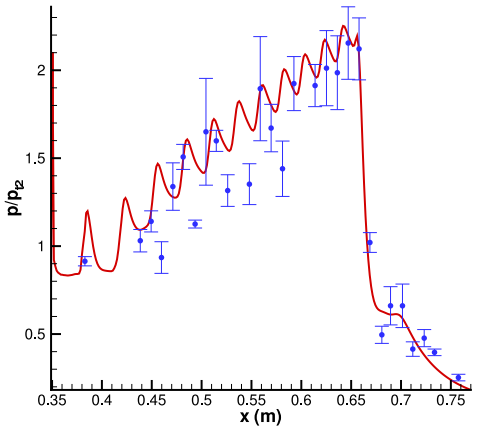

Figure 3. *Normalized pressure on the lower wall of simulated HyShot-II isolator/combustor. Lines: Present computations, Dots with error bars: DLR Measurements.*[6]

Table 1. Summary of parameters used in heat release model.

Symbol	Definition	Baseline value
ϕ	Equivalence ratio	0.3
f_{st}	Stoichiometric fuel/air ratio	0.028
H_f	Fuel heating value	$120\frac{MJ}{kgH_2}$
L_c	Combustor length	0.368m
K_c	Fraction of Completed combustion	0.95
D_c	Shape parameter	0.75
C_c	Shape parameter	$-log(1-K_c)^{D_c}$

can be used in the risk assessment procedure described in this work. When solved numerically on a mesh Ω_H, a discretized form of the governing equations $R_H(U_H, w) = 0$ is used to compute a discrete functional $\mathcal{J}(U_H, w)$. The variation of this discrete functional with respect to some change in the uncertain parameters δw is given by

$$\delta\mathcal{J} = \left(\frac{\partial\mathcal{J}}{\partial w} + \frac{\partial\mathcal{J}}{\partial U_H}\frac{\partial U_H}{\partial w}\right)\delta w. \tag{2}$$

This variation can be evaluated if $\frac{\partial U_H}{\partial w}$ is known, and this can be determined, for instance, by linearizing the governing equations $R_H(U_H, w) = 0$ and solving the resulting expression for $\frac{\partial U_H}{\partial w}$

$$\frac{\partial R_H}{\partial w} + \frac{\partial R_H}{\partial U_H}\frac{\partial U_H}{\partial w} = 0. \tag{3}$$

The above equation must be solved iteratively and the computational effort is comparable to solving the governing equation $R_H = 0$. Since Equation 3 has to be solved for every component w_i, this *direct* approach will be expensive if a large number of parameters are present in w . To circumvent this computational expense, the adjoint approach is useful; by introducing the adjoint variable Ψ as a Lagrange multiplier, we can write

$$\begin{aligned}\delta\mathcal{J} &= \left(\frac{\partial\mathcal{J}}{\partial w} + \frac{\partial\mathcal{J}}{\partial U_H}\frac{\partial U_H}{\partial w} + \Psi_H^T\left[\frac{\partial R_H}{\partial w} + \frac{\partial R_H}{\partial U_H}\frac{\partial U_H}{\partial w}\right]\right)\delta w,\\ &= \left(\frac{\partial\mathcal{J}}{\partial w} + \Psi_H^T\frac{\partial R_H}{\partial w}\right)\delta w,\end{aligned} \tag{4}$$

provided

$$\left[\frac{\partial R_H}{\partial U_H}\right]^T\Psi_H = -\left[\frac{\partial\mathcal{J}}{\partial U_H}\right]^T. \tag{5}$$

Equation 5 is called the *discrete adjoint* equation because its derivation proceeds directly from the discretized form of the governing equations. Note that, unlike Equation 3, Equation 5 does not contain derivatives with respect to w. This means that, irrespective of the dimension of w, we have to solve just one adjoint equation; the full gradient is then obtained from Equation 4 which only requires dot products and is hence computationally inexpensive. With this approach, the expense of computing the full gradient is roughly comparable to that of one additional flow solution. In this work, the software suite ADOL-C[11] has been used for automatic differentiation[12] of relevant routines.

A. Risk Quantification

Risk analysis for both the initial phase of the flight[13] and the overall trajectory,[14] as well as some aspects of the unstart control hardware[15] have previously been carried out for the X-43A hypersonic vehicle. These studies are based on simplified computational models which rely heavily on empirical correlations to predict

the system behavior. Uncertainties in the operating scenarios (atmospheric state, vehicle flight conditions, controls, etc. - namely aleatoric uncertainties[16]) were typically characterized using Gaussian probability distributions and propagated through the computational model using brute-force Monte Carlo sampling. In spite of the demonstrated success of this approach, there is a need to reduce the cost and effort involved in calibrating the computational models to allow a more comprehensive exploration of the design space and to extend the performance threshold closer to the operability limits by reducing excessively conservative use of the safety factors, while demonstrating reliability to expected variations in the operation of the vehicles.

In this work, we offer an alternative approach to reliability analysis in which the computational model includes a refined representation of the shock dynamics within the engine, but only a crude approximation to the mixing and combustion processes which are represented by a simplified heat-release model. Following the approach introduced by Iaccarino et al.,[17] instead of using empirical data to correlate the heat-release predictions, we introduce additional uncertain quantities such as the ignition location, amount of fuel burnt, etc, that do not represent the variability encountered during the operation of the actual vehicle (aleatory uncertainties) but rather indicate a *lack-of-knowledge* regarding the detailed physical processes (these are termed epistemic uncertainties[16]). In addition, the number of overall simulations required to investigate the probability of failure is reduced by using sensitivity information obtained through the use of adjoint methods. Sensitivity derivatives have been used before in hypersonic problems to help design SCRamjet inlets[2] leading to optimal geometrical shapes for the cowl and nozzles. The analyses were mainly based on analytical derivatives computed from quasi-1D thermodynamic equations. The connection between sensitivity derivatives and approximate representation of failure probability has been exploited in reliability estimate methods (see for example Ref.[18]); here we use the sensitivity information in an alternative way. Recently Wang[19] used the adjoint method to compute sensitivity derivatives and to formulate an acceleration strategy to concentrate Monte Carlo samples towards the tail of the output probability distributions. In this paper we apply this technique to the evaluation of the probability of unstart due to thermal choking.

IV. Formulation of the Risk Assessment Problem

The problem is to compute the probability that unstart is initiated in the SCRamjet engine, given probability distributions in the following five uncertaintain parameters:

1. Angle of attack of the vehicle,
2. Ambient temperature at a pressure altitude of 27,000 m,
3. Combustion shape parameter that describes the shape of the supersonic heat release in the combustor (D_c in eqn. 1),
4. Combustor burning fraction describing the percentage of fuel that is burnt in the combustor (K_c in eqn. 1), and
5. Combustor ignition position describing the position where the fuel first ignites, after the fuel injection at $0.408m$.

We denote this set of input uncertain parameters by the vector w.

A. Quantitative definition of unstart

Unstart in SCRamjet engines is characterized by the formation of a strong normal shock wave in the combustor. This shock wave propagates upstream towards the inlet and can significantly reduce the mass flow rate through the engine. The existence of the strong shock wave can be identified by sensing the difference between the maximum pressure in the combustor and the inlet pressure.

In practice, we find that a high-order polynomial norm of the combustor wall pressure serves as a very good approximation to the maximum pressure in identifying the existence of the unstart normal shockwave.

This metric is preferred because a polynomial norm is a smoother functional than the maximum norm, which in turn makes the functional gradient better behaved.

In this problem, we use the 8^{th} norm of the combustor upper-wall pressure (at a pre-specified simulation time) as the quantitative identifier of unstart. This functional is given by

$$\mathcal{J} = \left(\int_{W_U} (p - p_I)^8 ds \right)^{\frac{1}{8}}$$

where W_U denotes the upper wall of the combustor. This wall pressure is relative to the combustor inlet pressure p_I, and is normalized with respect to the inlet density ρ_I and the square of the velocity U_I of a reference configuration. The reference configuration is defined as the one that is achieved when all the uncertain input parameters take the the value of the mean of their respective distributions. Note that $\mathcal{J}$ is a function of w through the dependence of p on w expressed by the governing equations of the flow.

With this objective function $\mathcal{J}(w)$, we find that the value of

$$\mathcal{C} = 0.23$$

separates the operating SCRamjet cases and the unstart cases very cleanly (see Figure 6). Based on this observation, we define $\{w \mid \mathcal{J}(w) > \mathcal{C}\}$ as the region of the uncertain input parameter space that causes unstart, and $\{w \mid \mathcal{J}(w) < \mathcal{C}\}$ as the region of the uncertain input parameter space that ensures normal (or *started*) SCRamjet operation. Based on this criteria, the formal statement of the problem formulation is to calculate the unstart probability

$$\mathbb{P}\left(\{w \mid \mathcal{J}(w) > \mathcal{C}\}\right)$$

where the objective function $\mathcal{J}$ and the critical value $\mathcal{C}$ are defined as explained previously.

B. Probability distribution of uncertain input parameters

In this work, the chosen distributions of these uncertain parameters are summarized in Table 2 but the methodology described in this paper is able to handle arbitrary probability density functions that may be obtained from additional knowledge of the priors. These input parameters are assumed to be independent of each other. Figure 4 shows the probability density functions chosen for these parameters. We choose a

Table 2. Summary of input uncertain parameters.

Parameter	Mean	Standard dev	Probability distribution
Vehicle angle of attack α	0°	2°	Normal distribution
Ambient temperature T_A	223.5K	10.0K	Lognormal distribution with minimum 0K
Combustion shape parameter D_C	0.75	0.05	Beta distribution, bounded in $[0, 1]$
Combustion burning fraction K_C	0.95	0.03	Beta distribution, bounded in $[0, 1]$
Combustion ignition position X_C	0.418 m	0.010 m	Lognormal distribution with minimum 0.408 m
Ambient pressure p_A	Deterministic at pressure altitude of 27,000m – 2.188 kPa		
Freestream Mach number	Deterministic at Mach 7.5		

lognormal distribution for the ambient temperature T_A because the temperature (in degrees Kelvin) must be positive. Similarly, the position of ignition X_C must occur after the fuel injection, which is located at a distance of $0.408m$ from the nose of the entire vehicle. Therefore, we prescribe a lognormal random variable with a minimum value of $0.408m$. The combustor shape parameter D_C and burning fraction K_C are numbers between 0 and 1. Therefore, we use Beta distributions to describe these random variables.

Since the inflow to the computation domain corresponds to the flow after the forebody and cowl shocks, the uncertainties in the angle of attack and ambient temperature translate into uncertainties in the inflow pressure, density, temperature and velocity of the computation domain. The input uncertainties in these

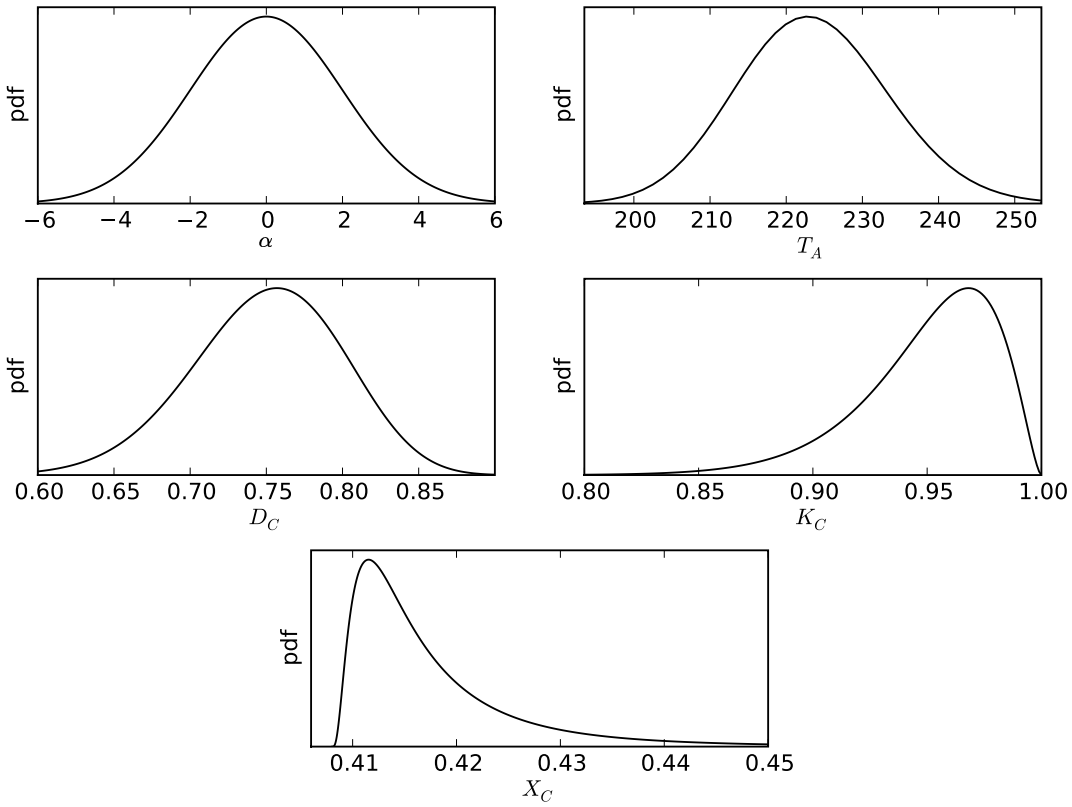

Figure 4. Probability density function of input uncertain parameters.

parameters are calculated by solving the oblique shock equation,[20] and non-dimensionalized to the reference velocity $1,882m/s$, the reference density $0.368kg/m^3$ and the reference pressure $1,223kPa$. The probability density functions of these inlet uncertain parameters, as input to the CFD calculation, are shown in Figure 5.

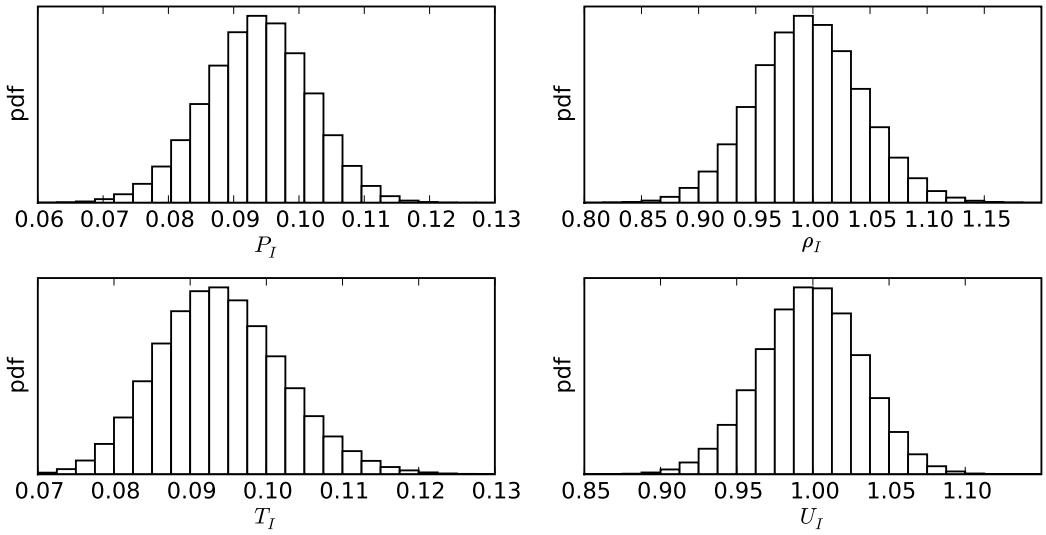

Figure 5. Empirical probability density function of uncertain parameters in the inflow condition, calculated from samples of α and T_A by solving the oblique shock equations twice.

V. Naïve Monte Carlo Method

The problem posed in the previous section can be solved using the naïve Monte Carlo method. The naïve Monte Carlo method takes N samples of the uncertain input parameters $w_1, \ldots, w_N$, and performs a flow solution for each sample. The objective function $\mathcal{J}(w_k)$ is then computed for each $k = 1, \ldots, N$. The probability of unstart is then estimated as the fraction of unstarted cases in the sampled simulations

$$\mathbb{P}(\mathcal{J}(w) > \mathcal{C}) \approx P_N^{mc} = \frac{1}{N} \sum_{k=1}^{N} I_{\mathcal{J}(w_k)>\mathcal{C}} \tag{6}$$

where

$$I_{\mathcal{J}(w)>\mathcal{C}} = \begin{cases} 1, & \mathcal{J}(w) > \mathcal{C} \\ 0, & \mathcal{J}(w) < \mathcal{C} \end{cases}.$$

Figure 6 shows a histogram of the objective function $\mathcal{J}(w_i)$ with $3,000$ samples. We can see from the plot that the critical value separates two distinct groups: the majority of the samples lie to the left of the critical value and are normal operating SCRamjets; a small portion of samples are seen to the right of the critical value. The high value of the objective function of these samples indicates the existence of strong normal shockwaves in the corresponding flow fields, as shown in Figure 7. The probability of unstart calculated using this naive Monte Carlo method for three different numbers of samples N is shown in Table 3.

Since the estimator P_N^{mc} in Equation (6) is an unbiased estimator, the only error comes from its variance. The variance of P_N^{mc} can be estimated by

$$Var(P_N^{mc}) = Var\left(\frac{1}{N}\sum_{k=1}^{N} I_{\mathcal{J}(w_k)>\mathcal{C}}\right) = \frac{Var\left(I_{\mathcal{J}(w_k)>\mathcal{C}}\right)}{N} \approx \frac{P_N^{mc} - P_N^{mc\,2}}{N}$$

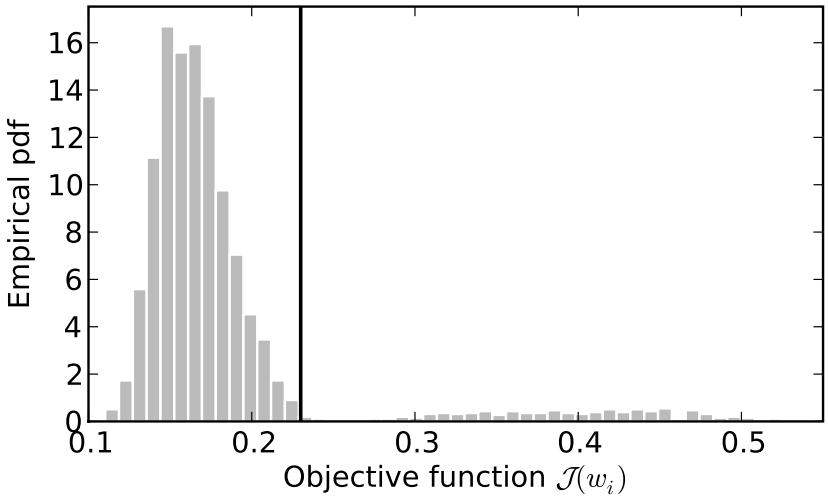

Figure 6. Empirical pdf of the objective function $\mathcal{J}$ based on 3,000 naive Monte Carlo samples. The vertical line indicates the critical value $\mathcal{C}$.

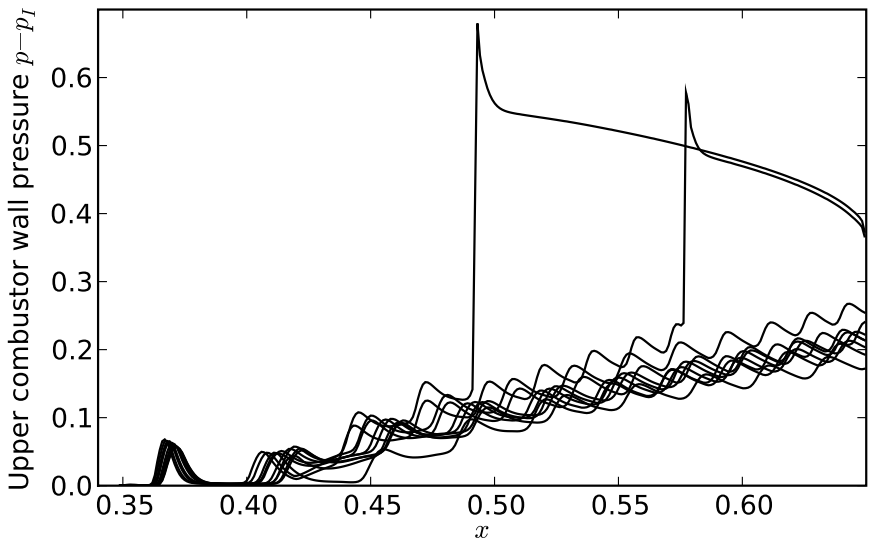

Figure 7. 10 random realizations of the combustor upper wall pressure. 8 samples are normal operating SCRamjets; the 2 samples with sharp peaks, indicating strong normal shockwaves in the combustor, are developing unstart.

Table 3. Summary statistics of naive Monte Carlo sampling

Number of samples	Estimated unstart probability	estimator variance	2σ confidence interval
1,000	0.073	6.8×10^{-05}	(0.057, 0.089)
2,100	0.083	3.6×10^{-05}	(0.071, 0.095)
3,000	0.082	2.5×10^{-05}	(0.072, 0.092)

This variance estimate, together with the resulting 2σ confidence interval of the unstart probability, is given in Table 3 for $N = 1000$, 2100 and 3000.

VI. Adjoint Approximation

Both the flow and the adjoint equations are solved at a reference condition w_0, where all the uncertain input parameters take on their respective mean values.

$$w_0 = F\big(\alpha_0, T_{A\,0}, D_{C\,0}, K_{C\,0}, X_{C\,0}\big) = F\big(0^\circ,\ 223.5K,\ 0.75,\ 0.95,\ 0.418m\big).$$

where F represents the solution of two oblique shock equations, which maps the uncertain input parameters to the uncertain inlet condition of the combustor. From the flow solution, we compute the objective function $\mathcal{J}(w_0)$. Using the adjoint solution, we can compute the derivative of the objective function $\mathcal{J}$ with respect to each uncertain input random variable. In other words, we compute the adjoint sensitivity gradient $\nabla\mathcal{J}(w_0)$. The computed sensitivity gradient is given in Table 4. With this adjoint sensitivity gradient, we construct a linear approximation to the objective function

$$\mathcal{J}(w) \approx \tilde{\mathcal{J}}(w) = \nabla\mathcal{J}(w_0) \cdot (w - w_0) + \mathcal{J}(w_0) \tag{7}$$

Table 4. Adjoint sensitivity gradient with respect to the uncertain inflow condition

Variable	K_C	D_C	X_C	ρ_I	p_I	T_I	U_I
Gradient	0.383	0.160	-0.593	-0.106	0.722	0.000	-0.413

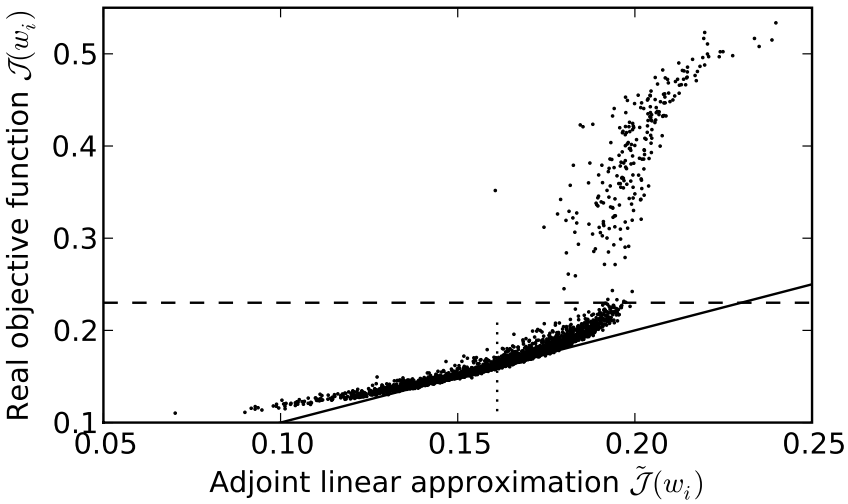

Figure 8. Adjoint approximation for the 3,000 naïve Monte Carlo samples, plotted against the real/computed value of the objective function. The solid line indicates the exact approximation $\mathcal{J} = \tilde{\mathcal{J}}$. The objective function of the reference configuration $\mathcal{J}(w_0) = \tilde{\mathcal{J}}(w_0)$ is indicated by the vertical dotted line.

This adjoint linear approximation $\tilde{\mathcal{J}}(w_i)$ for the samples $w_1, \ldots, w_{3,000}$ used in the last section is plotted in Figure 8 against the real objective function $\tilde{\mathcal{J}}(w_i)$. The linear approximation (based on one gradient evaluation) has an average of 20% error when the engine is in normal operation, and up to 150% error when the engine unstarts. The large error indicates strong nonlinearity in the problem, which is directly a consequence of the existence of strong non-linearities in the flow and the bifurcation nature of the unstart phenomenon.

Despite its limitations, the linear approximation correlates well with the real objective function, and is useful in identifying the trend. The configuration is much less likely to unstart when the linear approximation of $\tilde{\mathcal{J}}$ is small. When the linear approximation is large enough, the engine almost always experiences unstart. This observation is the key motivation for using the adjoint computed gradients to accelerate the Monte Carlo method for estimating the unstart probability $\mathbb{P}(\mathcal{J} > \mathcal{C})$, taking advantage of both the small computational cost of evaluating the adjoint approximation (7) and the strong correlation between $\tilde{\mathcal{J}}$ and $\mathcal{J}$.

VII. Adjoint-Based Stratified Sampling

A. Adjoint-based stratification

We separate the samples into three strata based on the adjoint linear approximation $\tilde{\mathcal{J}}$:

1. Safe stratum: in this group, the adjoint approximation predicts with high probability that the SCRamjet engine does not unstart.
2. Uncertain stratum: in this group, the adjoint approximation is unable to predict with confidence whether the SCRamjet engine unstarts or not.
3. Unstart stratum: in this group, the adjoint approximation predicts with high probability that the SCRamjet engine unstarts.

The boundaries of these three groups are determined by taking 100 preliminary samples of the uncertain parameters $w_1, \ldots, w_{100}$, and performing a flow solution on each of the 100 samples. From the flow solutions, the objective function $y_i = \mathcal{J}(w_i), i = 1, \ldots, 100$ is calculated. Based on whether this objective function exceeds the set threshold $\mathcal{C}$, the 100 preliminary samples are categorized into safe and unstart samples.

The adjoint approximation of the objective function, $x_i = \tilde{\mathcal{J}}(w_i), i = 1, \ldots, 100$ is also computed for these 100 samples. For both the safe and unstart samples, we compute the mean and standard deviation. In other words, we compute the sample mean μ_{x1} and standard deviation σ_{x1} of $\{x_i | y_i < \mathcal{C}\}$, and the sample mean μ_{x2} and standard deviation σ_{x2} of $\{x_i | y_i > \mathcal{C}\}$.

Based on the mean and standard deviation of these two groups, we define the boundary between the three strata for the stratified sampling algorithm. The safe stratum is defined as

$$S_1 = \{w | \tilde{\mathcal{J}}(w) < \mu_{x2} - 2\sigma_{x2})\} ;$$

the unstart stratum is defined as

$$S_3 = \{w | \tilde{\mathcal{J}}(w) > \mu_{x1} + 2\sigma_{x1}\} ;$$

and the uncertain stratum is defined as

$$S_2 = \{w | \mu_{x2} - 2\sigma_{x2} < \tilde{\mathcal{J}}(w) < \mu_{x1} + 2\sigma_{x1}\} .$$

The stratification scheme is illustrated in Figure 9. The resulting stratification is given in row 3 of Table 5.

B. Calculation of the unstart probability

The following three steps are used to calculate the unstart probability using our adjoint-based stratified sampling:

1. Calculate the probability that a sample falls into each stratum,

   $$\mathbb{P}(w \in S_i) \ , \ i = 1, 2, 3.$$

   These probabilities are calculated by computing the adjoint approximation for $N_A = 13,160,000$ samples w, and determining the fraction of samples that lie in each stratum S_i.

   $$\mathbb{P}(w \in S_i) \approx P_i^{(1)} = \frac{1}{N_A} \sum_{k=1}^{N_A} I_{w_k \in S_i} \ , \ i = 1, 2, 3. \tag{8}$$

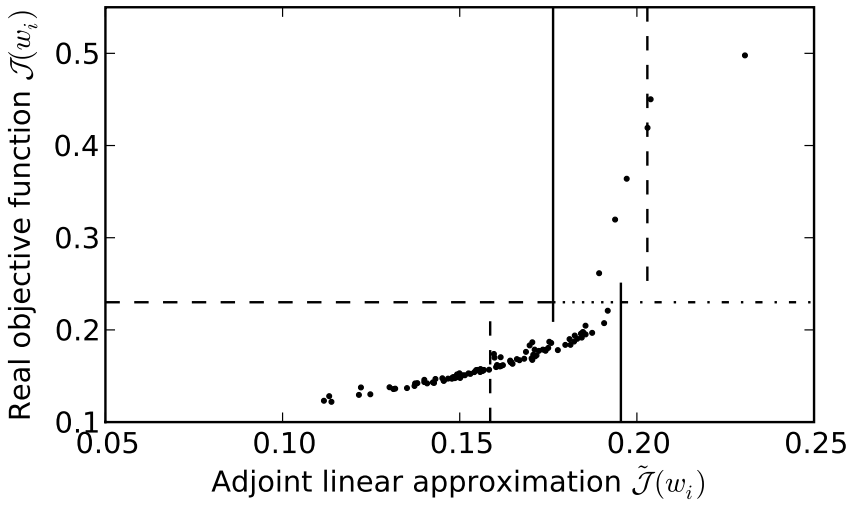

Figure 9. Stratification scheme using flow solutions and adjoint approximations of 100 samples. The dots represent the 100 Monte Carlo samples. The horizontal line indicates the boundary between operating safe and unstart cases. The lower left vertical dash line indicates the sample mean of the adjoint approximation $\tilde{\mathcal{J}}$ of the operating cases; the upper right vertical dash line indicates the sample mean of the adjoint approximation $\tilde{\mathcal{J}}$ of the unstart cases. The lower solid vertical line indicates the right two-standard-deviation boundary of the operating cases; the upper solid vertical line indicates the left two-standard-deviation boundary of the unstart cases. These two solid lines separate the sample space into three strata based on the adjoint approximation: the dashed part of the horizontal line indicates Stratum 1, the safe stratum; the dotted part of the horizontal line indicates Stratum 2, the uncertain stratum; the dash-dot part of the horizontal line indicates Stratum 3, the unstart stratum.

where

$$I_{w_k \in S_i} = \begin{cases} 1, & w_k \in S_i \\ 0, & w_k \notin S_i \end{cases} .$$

Because each stratum is defined in terms of the adjoint approximation $\tilde{\mathcal{J}}$, calculating the probabilities involves only sampling the uncertain parameters w, and calculating the adjoint linear approximation $\tilde{\mathcal{J}}$. Since the computational cost of sampling $\tilde{\mathcal{J}}$ is negligible compared to sampling $\mathcal{J}$, we can use as many samples as necessary to keep the error in the calculated $\mathbb{P}(w \in S_i)$ under a desired level.

In our calculations, we used $13,160,000$ samples to calculate these probabilities. As shown in Section C, the resulting statistical variances in these probability estimates are orders of magnitude lower than the variance in the conditional probability calculated in Step 2. Therefore, the errors in the computed probabilities are negligible in our analysis. The calculated probabilities and variance estimates are given in Rows 4 and 5 of Table 5.

2. Calculate the conditional probability of unstart, given that a sample falls into each stratum

$$\mathbb{P}(\mathcal{J}(w) > \mathcal{C} \mid w \in S_i) \ , \ i = 1, 2, 3.$$

We perform flow solutions on $2,000$ samples. The number of samples in the three strata N_1, N_2, N_3 is chosen to be proportional to the probability of the stratum, calculated in Step 1. The samples $w_k^i, k = 1, \ldots, N_i, i = 1, 2, 3$ are generated by obtaining a large number of samples and selecting the first N_i samples that lie in stratum i.

The conditional probability of unstart occurring in each stratum is estimated as the fraction of unstarted

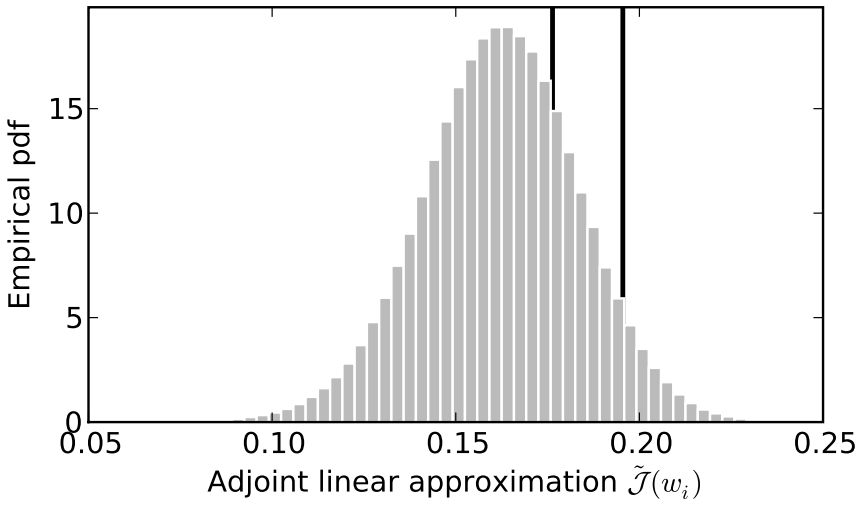

Figure 10. Calculating the probability of each stratum by calculating the adjoint linear approximation of $13,160,000$ samples. The gray histogram shows the empirical pdf derived from the large number of samples. The two vertical lines show the boundary between the three strata.

cases in that stratum. In other words, we estimate

$$\mathbb{P}(\mathcal{J}(w) > \mathcal{C} \mid w \in S_i) \approx P_i^{(2)} = \frac{1}{N_i} \sum_{k=1}^{N_i} I_{\mathcal{J}(w_k^i)>\mathcal{C}} \tag{9}$$

where

$$I_{\mathcal{J}(w_k)>\mathcal{C}} = \begin{cases} 1, & \mathcal{J}(w_k) > \mathcal{C} \\ 0, & \mathcal{J}(w_k) < \mathcal{C} \end{cases}.$$

The number of samples in each stratum N_i, the number of unstarted solutions, and the calculated conditional probabilities are shown in Rows 6, 7 and 8 of Table 5.

3. Calculate the probability of unstart

$$\mathbb{P}(\mathcal{J}(w) > \mathcal{C}) = \sum_{i=1}^{3} \mathbb{P}(w \in S_i)\, \mathbb{P}(\mathcal{J}(w) > \mathcal{C} \mid w \in S_i) \approx P^{ss} = \sum_{i=1}^{3} P_i^{(1)} P_i^{(2)} \tag{10}$$

This probability estimate is shown in Row 11 of Table 5.

C. Confidence interval of unstart probability estimates

We first analyze the error in estimator $P_i^{(1)}$ in Equation 8. Since $\mathbb{P}(w \in S_i) = \mathbb{E}(I_{w_k \in S_i})$, the estimator is unbiased, and the error is solely from the variance:

$$Var(P_i^{(1)}) = Var\left(\frac{1}{N_A} \sum_{k=1}^{N_A} I_{w_k \in S_i}\right) = \frac{Var(I_{w \in S_i})}{N_A} = \frac{\mathbb{P}(w \in S_i) - \mathbb{P}(w \in S_i)^{(2)}}{N_A} < 1.9 \times 10^{-8}$$

for $N_A = 13,160,000$. This is negligible compared to the variance of estimating the conditional probabilities, as shown in Table 5.

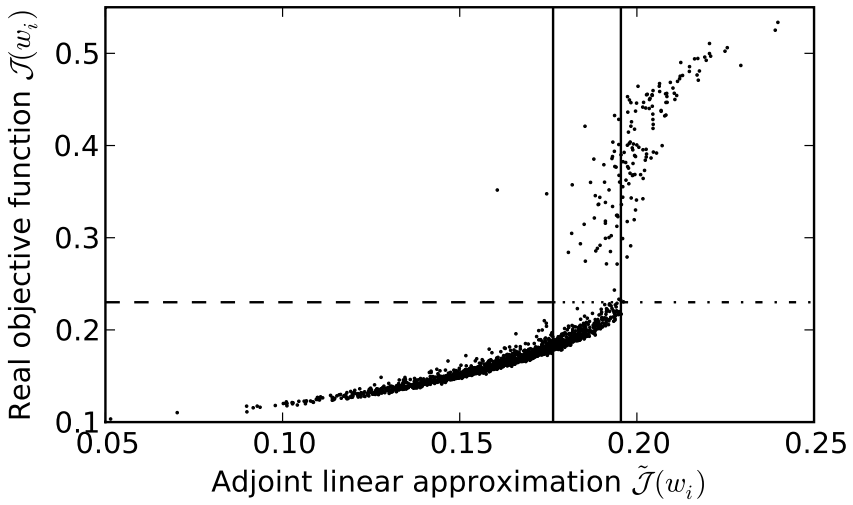

Figure 11. Stratified sampling with actual flow solutions on 2,000 samples. The horizontal line indicates the boundary between operating/started cases and unstarted cases. The vertical lines indicate the boundaries between the three strata: the dashed part of the horizontal line indicates Stratum 1, the started stratum; the dotted part of the horizontal line indicates Stratum 2, the uncertain stratum; the dash-dot part of the horizontal line indicates Stratum 3, the unstart stratum.

Following this, we estimate the error in the estimator $P_i^{(2)}$ of the conditional probabilities in Equation (9). It is also an unbiased estimator, and the variance is

$$Var(P_i^{(2)}) = Var\left(\frac{1}{N_i}\sum_{k=1}^{N_i} I_{\mathcal{J}(w_k^i)>\mathcal{C}}\right) = \frac{Var\left(I_{\mathcal{J}(w_k^i)>\mathcal{C}}\right)}{N_i} \approx \frac{P_i^{(2)}(1-P_i^{(2)})}{N_i}\,.$$

Row 9 in Table 5 shows the variance of these conditional probability estimations.

When we neglect the small randomness in the estimated $\mathbb{P}(w \in S_i)$, the estimate of the unstart probability by Equation (10) is unbiased. Because the samples in each stratum are independent, the variance of the estimator in Equation (10) is

$$Var\left(\sum_{i=1}^{3}\mathbb{P}(w\in S_i)\,\mathbb{P}(\mathcal{J}(w)>\mathcal{C}\mid w\in S_i)\right).$$

From Table 5, we see that the stratified sampling algorithm has greatly reduced the variance compared to the naïve Monte Carlo simulation with the same number of flow solutions as shown in Table 3. As can be seen in the table, the total variance of the stratified sampling is reduced to 31% that of the naive Monte Carlo method with $2,100$ flow solutions, shown in Table 3. The naïve Monte Carlo method would need about $6,600$ samples in order to achieve the same level of variance. Therefore, the adjoint-based stratified sampling scheme has been shown to accelerate the Monte Carlo method by a factor of more than 3.

VIII. Optimal Allocation for Stratified Sampling

The efficiency of the adjoint based stratified sampling scheme can be further improved by optimally allocating the number of flow solutions within each stratum. The optimal number of samples for each stratum can be calculated by solving the constrained optimization problem

$$\min_{N_i} Var(P^{ss}) = \sum_{i=1}^{3}\mathbb{P}(w\in S_i)^2\,\frac{P_i^{(2)}(1-P_i^{(2)})}{N_i} \quad \text{s.t.} \quad \sum_{i=1}^{3} N_i = N.$$

Table 5. Summary statistics of adjoint based stratified sampling computation

Stratus	Started	Uncertain	Unstart
i	1	2	3
$\{\tilde{\mathcal{J}}(w) \mid w \in S_i\}$	$(-\infty, 0.17635)$	$(0.17635, 0.19548)$	$(0.19548, +\infty)$
$P_i^{(1)} \approx \mathbb{P}(w \in S_i)$	0.74741	0.19521	0.05738
Variance of $P_i^{(1)}$	$< 1.9 \times 10^{-8}$	$< 1.9 \times 10^{-8}$	$< 1.9 \times 10^{-8}$
number of flow solutions N_i	1495	390	115
number of unstart flow solutions	2	48	114
$P_i^{(2)} \approx \mathbb{P}(\mathcal{J}(w) > \mathcal{C} \mid w \in S_i)$	0.0014	0.123	0.9913
Estimator variance of $P_i^{(2)}$	8.9×10^{-7}	0.000277	0.000075
Contribution to the variance of P^{ss}	5.0×10^{-7}	1.05×10^{-5}	2.5×10^{-7}
$P^{ss} \approx \mathbb{P}(\mathcal{J}(w) > \mathcal{C})$	0.082		
Estimator variance of P^{ss}	1.13×10^{-5}		
2σ confidence interval of P^{ss}	$(0.075, 0.089)$		
Total number of flow solutions	2,100		

Here we minimize the total variance as the cost function, given that the total number of flow solutions is fixed. Using the Lagrange multiplier method, we take the derivative of the cost function and the constraint with respect to N_i, and obtain the following relation

$$\mathbb{P}(w \in S_i)^2 \, \frac{P_i^{(2)}(1 - P_i^{(2)})}{N_i^2} = \lambda.$$

In other words, the optimal number of flow solutions in each domain should be proportional to

$$N_i \propto \mathbb{P}(w \in S_i) \sqrt{P_i^{(2)}(1 - P_i^{(2)})} \tag{11}$$

According to this formula, we calculated the optimal fraction of flow solutions in each stratum. The numbers are shown in Row 3 of Table 6.

On top of the 2,100 flow solutions that were performed in the last section, we now perform 900 additional flow solutions to further decrease the error in our estimation of the unstart probability. We allocate these additional flow solutions so that the total number of flow solutions in each stratum is as close as possible to the optimal fraction. The resulting number of additional flow calculations in each stratum is given in Row 5 of Table 6. Figure 12 shows the histogram of the adjoint approximation $\tilde{\mathcal{J}}$ of the existing as well as the additional flow solutions. We can see from the table and the plot that most of the additional flow solutions are allocated in the uncertain stratum. This is because the uncertainty in this stratum, reflected by the variance of an individual sample $P_i^{(2)}(1 - P_i^{(2)})$, is highest.

Table 6 summarizes the computation of the unstart probability and its variance. By performing only 900 additional calculations, the variance is reduced to 41% of that produced in the previous section. Compared to adding the same number of flow solutions but with the same sub-optimal allocation strategy, the optimal allocation strategy further accelerated the Monte Carlo sampling method by 67%. Compared to the naive Monte Carlo method with $3,000$ flow solutions, the adjoint based stratified sampling algorithm with optimal allocation reduces the variance to 18.6% that of naive Monte Carlo. In other words, it accelerated Monte Carlo sampling by a factor of 5.4.

IX. Conclusions & Future Work

This study demonstrates an adjoint-based approach for accelerating Monte Carlo estimations of risk. The approach is applied to estimating the unstart probability of a SCRamjet engine under uncertain conditions.

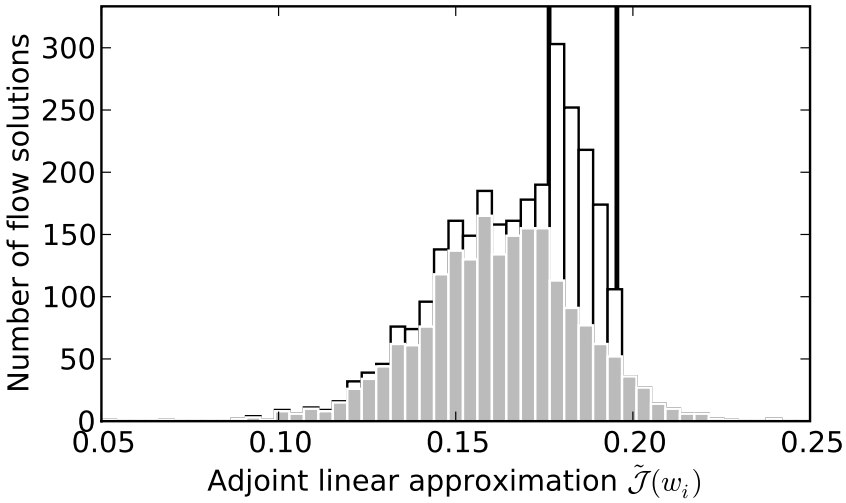

Figure 12. Histogram of $\tilde{\mathcal{J}}$ for existing and additional flow solutions. The gray bars indicates existing flow solutions; the white bars on top of the gray bars indicate additional flow solutions. The two vertical lines indicate the boundary between the three strata.

Table 6. Summary statistics of optimal allocation for adjoint based stratified sampling

Stratus i	Safe 1	Uncertain 2	Unstart 3
Optimal sample fraction based on Equation (11)	0.6142	0.3766	0.0092
Existing number of flow solutions	1495	390	115
Additional flow solutions	231	669	0
Total flow solutions	1726	1059	115
Total number of unstart flow solutions	2	136	114
$P_i^{(2)} \approx \mathbb{P}(\mathcal{J}(w) > \mathcal{C} \mid w \in S_i)$	0.0012	0.128	0.9913
Estimator variance of $P_i^{(2)}$	6.7×10^{-7}	0.000106	0.000075
Contribution to the variance of P^{oa}	3.7×10^{-7}	4.03×10^{-6}	2.5×10^{-7}
$P^{oa} \approx \mathbb{P}(\mathcal{J}(w) > \mathcal{C})$	0.083		
Estimator variance of P^{oa}	4.65×10^{-6}		
2σ confidence interval of P^{oa}	$(0.079, 0.087)$		
Total number of flow solutions	3,000		

The uncertainty is described by five random input parameters with various Gaussian and non-Gaussian distributions. Unstart can be identified by the existence of a strong normal shock wave in the combustor, creating a large pressure peak on the combustor wall. In this study, We define the objective function $\mathcal{J}$ as the 8th norm of the upper combustor wall, and quantitatively determine unstart as the objective function exceeding a certain critical value.

The adjoint equation is solved with respect to the objective function $\mathcal{J}$ and the adjoint solution is used to generate a linear approximation to the objective function. Due to the strong nonlinearities in the problem, the linear approximation can be inaccurate in regions of the parameter space that are "distant" from the linearized state. Nevertheless, this adjoint linear approximation is computationally inexpensive to evaluate, and correlates well with the true value of the objective function. These two characteristics enables variance reduction of Monte Carlo method based on the linear approximation.

Adjoint-based stratified sampling has been applied to reduce the variance of our estimate of the unstart probability. The sample space of the uncertain input parameters is divided into three different strata (corresponding to safe operation of the engine, uncertain operation and unstart) based on the adjoint linear approximation. The probability of unstart within these strata is very different and as a result, stratified sampling-based on these strata significantly reduces the variance of the estimator. We further calculate the optimal fraction of flow calculations within each stratum. Stratified sampling with optimal allocation of samples further reduces the variance of the estimator. Using the adjoint based variance reduction technique, the Monte Carlo method was demonstrated to be accelerated by a factor of 5.4.

The addition of higher-order derivatives computed using discrete adjoints could further enhance the efficiency of this method. Such an approach will be investigated in future work.

Acknowledgments

This work was funded by the United States Department of Energy's Predictive Science Academic Alliance Program (PSAAP) at Stanford University.

References

[1]Rausch, V.L., McClinton, C.R., Sitz, J. and Reukauf, P., "NASA's Hyper-X Program," *51st International Astronautical Congress, October 2000, Rio de Janeiro, Brazil*, 2000.

[2]Mayer, D.W. and Paynter, G.C. "Prediction of Supersonic Inlet Unstart Caused by Freestream Disturbances," *AIAA-1994-0580*, 1994.

[3]Star, J.B., Smart, M.K., Edwards, J.R., and Baurle, R.A., "Investigation of Scramjet Flow Path Instability in a Shock Tunnel," *AIAA-2006-3040*, 2006.

[4]Pecnik, R., Terrapon, V., Ham, F., and Iaccarino, G., "Full System Scramjet Simulation," Annual Research Briefs of the Center for Turbulence Research, Stanford University, 2009.

[5]Smart, M., Hass, N., and Paull, A., "Flight Data Analysis of the HyShot 2 Scramjet Flight Experiment," *AIAA Journal*, **44**, pp. 2366-2375, 2006.

[6]Schramm, J.M., Karl, S., Hanneman, K., and Steelant, J., "Ground Testing of the HyShot II Scramjet Configuration in HEG," AIAA Paper 2008-2547, 2008.

[7]Doolan, C.J., Boyce, R.R., "A Quasi-One-Dimensional Mixing and Combustion Code for Trajectory Optimisation and Design Studies," AIAA Paper 2008-2603, 2008.

[8]Jameson, A., "Aerodynamic Design via Control Theory," *J. of Scientific Computing*, Vol. 3, 1988, pp. 233–260.

[9]Giles, M., and Pierce,N., "Adjoint Equations in CFD: Duality, Boundary Conditions and Solution Behaviour," AIAA Paper 97-1850, 1997.

[10]Giles, M., Duta, M., Müller, J-D. & Pierce, N., "Algorithm Developments for Discrete Adjoint Methods," *AIAA Journal* Vol. **41**(2), 198-205, 2003.

[11]Griewank, A., Juedes, D., and Utke, J., "Algorithm 755: ADOL-C: A Package for the Automatic Differentiation of Algorithms Written in C/C++," *ACM Transactions on Mathematical Software*, **22**(2), pp. 131-167, 1996.

[12]Griewank, A., *Evaluating Derivatives, Principles and Techniques of Algorithmic Diferentiation.*, Society for Industrial and Applied Mathematics, Philadelphia, 2000.

[13]Lien, J., Bose, D., and Martis, J.G., "Automated Sensitivity Analysis of Hyper-X (X-43A) Separation Simulation," *AIAA-2004-4930*, 2004.

[14]Baumann, E., Beck, R., and Richard, M., "The X-43A Six-Degree of Freedom Monte Carlo Analysis," *AIAA-2008-0203*, 2008.

[15]Huebner, L.D., Rock, K.E., Ruf, E.G., Witte, D.W., and Andrews, E.H., "Hyper-X Flight Engine Ground Testing for X-43 Flight Risk Reduction," *AIAA-2001-2803*, 2001.

[16]Trucano, T., "Prediction and Uncertainty in Computational Modeling of Complex Phenomena: A Whitepaper. Sandia National Laboratories," *Report SAND98-2776*, 1998.

[17]Iaccarino, G., Pecnik, R., Glimm, J., and Sharp, D., "A QMU Approach to Characterizing the Operability Limit of air-breathing hypersonic vehicles," submitted to Reliability Engineering System Safety.

[18]Giunta, A.A., Eldred, M.S., Swiler, L.P., Truncano, T.G., and Wojtkiewicz, S.F., "Perspective on Optimization Under Uncertainty: Algorithms and Applications," *AIAA-2004-4451*, 2004.

[19]Wang, Q., *Uncertainty Quantification for Unsteady Fluid Flow using Adjoint-based Approaches*, Ph.D. thesis, Stanford University, Stanford, CA, 2009.

[20]Liepmann, H. W. and Roshko, A., *Elements of gas dynamics*, Wiley, New York, 1957.

[21]Wang, Q., Iaccarino, G., Ham, F. and Moin, P. "Risk Quantification in Unsteady Flow Simulations using Adjoint-based Approaches," *AIAA-2009-2277*, 2009.